STEADY-STATE ACCELERATION OF ALKALI PLASMA IN EXTERNAL CROSSED ELECTRIC AND MAGNETIC FIELDS

G. B. Babkin, S. D. Grishin,
V. A. Zhirnov, S. S. Kellin,
and A. V. Potapov

UDC 538.4

The results of an experimental investigation of the electromagnetic acceleration of an alkali plasma in single- and double-stage E,H-accelerators are discussed. The nature of the discharge in accelerators with ceramic and metallic walls is investigated. The number of elements of the metallic wall necessary for preventing breakdown is determined. The thrust and efficiency of different constructions are determined, and their efficiencies and effectiveness are compared.

The problems related to the theoretical and experimental investigations of different types of plasma accelerators of steady-state action have been discussed most thoroughly in [1]. However, in this work the authors have not discussed the physically interesting scheme of a continously operating plasma accelerator with crossed external electric and magnetic fields, in which condensing, easily ionizable substances, in particular, alkali metals, are used as the operating substance. The articles on E,H-accelerators, published in periodicals in recent years [2, 3], are devoted to the investigation of relatively cold, weak-current constructions operating with gases (argon) without an autonomous plasma source and are characterized by instability of the operating process with a sharp divergence of the electron temperature T_e from the ion temperature T_i and neutron temperature T_n ($T_n/T_e \leq 2\cdot 10^{-2}$), low flow velocity ($\leq$2 km/sec), and large values of the Hall parameter ($\omega_e\tau_e >> 1$) along the entire channel. Therefore, these systems are inefficient, have short lives, and are not very promising from the practical point of view.

The E,H-accelerators of alkali metal plasma with independent plasmotron and profiled magnetic field, investigated in the present work, are very promising for the optimization of the operating process of acceleration. In particular, the use of alkali metals permits one to improve both the ionization state in the accelerator channel and the thermionic emission characteristics of the electrodes. Low-voltage electric supply sources can be used for ensuring their operation; the required capacity of the vacuum equipment in bench conditions is considerably lower than in the case when gases are used. In conjunction with a number of special technical solutions, for example, organization of multistage plasma acceleration and control of the thermal regime of the accelerator channel, and with the current progress in the technology of superconducting magnetic systems these useful qualities make this system very attractive, and it merits the attention of investigators.

However, in spite of its advantages until recently a number of problems of physics and technology of steady-state acceleration of metallic plasma in E,H-fields had not been investigated experimentally. Thus, the verification of the efficiency of the electromagnetic accelerator, the investigation of the possibility of obtaining distributed discharge over a relatively large area of the electrodes, study of the durability of the electrodes, etc., had to be carried out.

In the present article we discuss experimental results which permit us to make some valid inferences about the basic characteristics of the operating process of an E,H-ac-

Moscow. Translated from Zhurnal Prikladnoi Mekhaniki i Tekhnicheskoi Fiziki, No. 6, pp. 20-30, November-December, 1974. Original article submitted May 21, 1974.

celerator of alkali plasma and determine ways of refining it.

1. Description of the Experiment

The experiments were conducted on models of accelerator channels of two types differing mainly in the geometry and the thermal regime. The first type, a low-temperature model (LTM) [Fig. 1a; 1) magnetic coils, 2) lateral dielectric walls, 3) anode, 4) cathode], is characterized by a constant cross section of the channel and relatively low temperatures of directly heated electrodes (1300-1500°K); a liquid eutectic alloy of sodium and potassium is used as the main operating substance.

The characteristic feature of the second scheme, the high-temperature model (HTM), is a channel diverging toward the exit and a figured construction of the directly heated electrodes (Fig. 1b; notations are the same as in Fig. 1a) ensuring a uniform heating of the operating segment swept by the plasma to a high temperature (2500-2700°K); in order to compensate for the thermal expansion of the electrodes during heating the connection of one of the current-carrying wires of each electrode was made from a soft element. The layer of ZrO_2 by the plasma method; lithium was mainly used as the operating substance; a eutectic alloy of sodium, potassium, and cesium was used in some isolated experiments.

Continuous and segmented electrodes (Fig. 1a) were used in the construction of the LTM channel; in special investigations a channel of constant cross section and a two-stage scheme consisting of two successive accelerator chambers were investigated as variants of the HTM.

The LTM channel had a transverse cross section of 40×40 mm^2 and a length $L = 300$ mm. In the main variant of single-stage HTM I the width of the channel was 30 mm, height 20 mm (entrance) and 40 mm (exit), and $L = 200$ mm. In the two-stage HTM II the dimensions of the channel of the first (from the plasma source) section were: width 30 mm, height at entrance 20 mm, height at exit 40 mm, length of the cathode 150 mm; the dimensions for the second section were: width 30 mm, height at entrance 40 mm, height at exit 60 mm, length of the cathode 150 mm. The electrodes were made of plates and ribbons (thickness $\delta \leq 1$ mm) of molybdenum, tungsten, and alloys of molybdenum–rhenium MR47, MR08, and tungsten–rhenium TR27. As the lateral walls of the models in the initial experiments electrical plates made of boron carbonitride (BCN), boron alumonitride (BAN), and quartz were used.

The magnetic system of the models consisted of two solenoid coils (1) placed near the side walls and of special inserts of a magnetic material (Armco) with which a profiled magnetic field decreasing toward the exit was produced. Typical profiles of the magnetic field B are shown in Fig. 2 (continuous curves — LTM, dashed curves — HTM 1). This magnetic system ensured values of the Hall parameter $\omega_e\tau_e$ of the order of 1-2 in the plasma over the main length of the accelerator channel. Below, the maximum value of the magnetic induction is denoted by B_M.

The alkali metal plasma was formed and fed to the accelerator channels of the LTM and HTM by electric-arc sources of type [4-6] in the range of mean mass flow of the operating substance 0.005-0.05 g/sec with power consumption of 2-6 kW. The tests of the HTM were carried out in a cooled vacuum space of ~20 m^3 at an operating pressure of ~10^{-4} mm Hg. The LTM samples were investigated in a cooled vacuum chamber (volume ~1.5 m^3) keeping the pressure during the experiment at 10^{-3}-10^{-2} mm Hg.

2. Procedure of Measurements

Along with the standard measurements of the electrical parameters of the models (currents, voltages), recorded continuously on N700, N004M, N105 loop oscillographs, special measurements of a number of characteristics of the operating process were also made.

The temperature of the operating surfaces (of electrodes, side walls) was recorded with an OPPIR-017 optical pyrometer (accuracy of temperature measurement 10%) and with thermocouples (Chromel–Alumel or tungsten–rhenium) depending on the value of the measured temperature. Probe and spectroscopic methods were used for measuring the plasma parameters (potential, electron concentration n_e, electron temperature T_e, velocities of the neutral and ionized components of the plasma, and the temperature of heavy particles).

Plane and cylindrical Langmuir probes were placed inside the accelerator channels (for recording the transverse and longitudinal profiles), as well as at the entrance and exit. The plane probes were in the form of a tantalum plate of 0.2 mm thickness and 1 mm diameter. The disks were welded to tantalum wires with ϕ = 0.5 mm. The area of the disk lying on the opposite side of the welded wire holder served as the collecting surface; the nonoperating plane of the disk and the surface of the wire were coated with an insulating ZrO_2 layer by the plasma-deposition method. The cylindrical probes were made from tungsten wire with ϕ = 0.2-0.3 mm embedded in a BNTs dielectric tube except for the collecting surface. The ion velocity was measured by the directional-probe method, according to which the collecting surface of one of the two probes was placed parallel to the flow and the other perpendicular (up to 12 pairs of probes were used along the accelerator channel).

The analysis of the data for obtaining the probe characteristics was done using the well-known formulas [7, 8]. The error in the measurement of T_e was 20-25%, while for n_e it was 20-30%. Side by side with the probe measurements the electron temperature was also determined by the spectroscopic method of relative intensities (Orshtein method) of the lines LiI λ 4132.29 Å and λ4273.28 Å, λ 4132.29 Å and λ 4971.99 Å using transition probabilities from [9, 10]. The required verification of the validity of Boltzmann energy distribution of the particles was done as usual by plotting in $I_s\lambda/Ag$ as a function of the excitation energy of the upper level (I_s is the relative intensity of the line, λ is wavelength, A is the transition probability, and g is the statistical weight of the level).

The electron concentration was measured spectroscopically from Stark broadening of the spectral line of the diffuse series Li I λ 4132.29 Å (linear Stark effect) with 15-20% accuracy [11]. In order to determine the velocity of the directed flow of neutral particles by the Doppler effect the emission of the LiI λ 4132.20 Å or λ 4273.28 Å lines along the two channels (normal to the plasma flow and making an angle of 30° with the flow) was measured and was directed to the slit of the spectrograph with a system of mirrors and condensers. A UV-84 camera with a UV-63 collimator mounted on an ISP-51 spectrograph served as the radiation receiver. The light fluxes were spaced along the height of the slit by a total internal-reflection prism inserted into the collimator. In some experiments the averaged values of n_e and T_e were determined by SHF diagnostics.

The momentum of the plasma jet at the exit of the channel was measured systematically (50-80 mm from the end face) with a collector-balance suspended on thin elastic ribbons or prismatic supports. The signal from the displacement of the balance under the action of the reaction force of the outflowing plasma jet was picked up with an inductive sensor in which thin membranes were used as the elastic element, and it was recorded on the strip chart of an electronic automatic recording potentiometer EPP-09M. The sensor was fed from an acoustic oscillator with a calibration curve taking into account the error associated with the heating of the system.

3. Results of Experiments on Models with Ceramic Walls

In a number of experiments with LTM with ceramic walls made of BNTs (thickness 10 mm) using lithium plasma without special preheating of the electrodes from external sources, and also with relatively weak preheating of the cathode (temperature of the cathode $T_c \leq$ 700-800°K), it was found that the discharge had the form of an unstable electric arc occupying a small part of the channel; besides, an intensive condensation of lithium was observed on relatively cold inner surfaces of the dielectric walls (the temperature of the walls on the side of the plasma $T_w \leq 600$°K). The heating of the molybdenum cathode from an independent dc generator up to T_c = 1300-1500°K made it possible to somewhat stabilize the discharge and to eliminate the condensation of lithium to a large extent; however, a complete homogeneity of the discharge current over the electrode could not be obtained, and the volt-ampere characteristics (for parallel connection of the three segments of the anode if segmented) had a slightly decreasing character both in the presence and absence of the magnetic field. The volt-ampere characteristics of the discharge in the LTM are shown in Fig. 3, where data 1-7 correspond to the following conditions: 1) eutectic alloy of sodium and potassium, $\dot{m}$ = 0.02 g/sec, metallic walls; 2) first segment of the anode, B_M = 2350 G; 4) solid anode, B_M = 0; 5) lithium, $\dot{m}$ = 0.032 g/sec, ceramic walls; 6) B_M = 1000 G; 7) B_M = 700 G.

In spite of the clearly unfavorable situation in the LTM channel an increase of the reaction P compared to the plasmotron was noted. Thus, the following parameters of the plasma source were recorded in the steady-state regime: flow rate of lithium $\dot{m}$ = 0.032

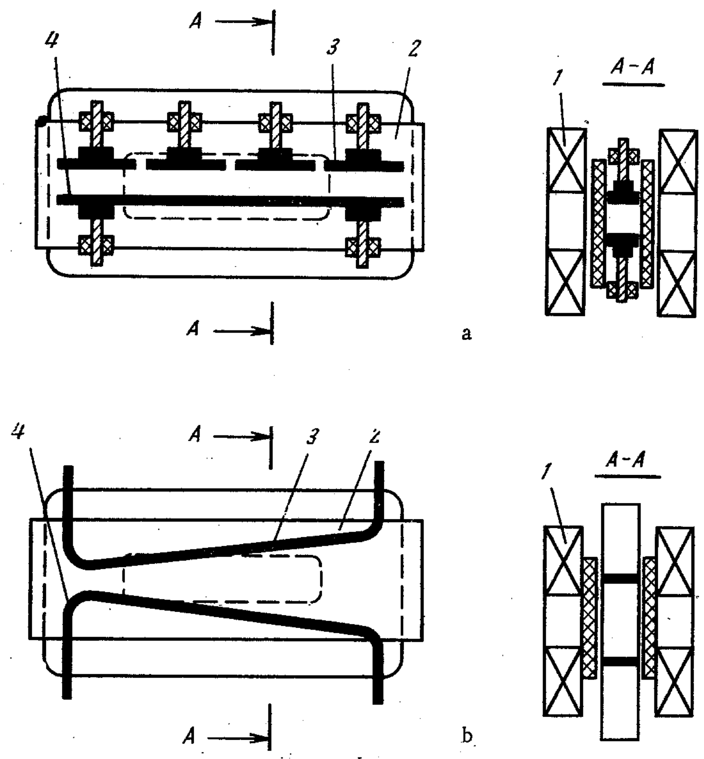

Fig. 1

g/sec, discharge voltage U_p = 15 V, discharge current L_p = 300 A, P = 11 g, v = 3 km/sec, $T_e \approx 6500°K$, $T_n \approx 4500°K$. The parameters of the LTM channel were: B_M = 3560 G, T_c = 1200°K, $T_w \approx 1000°K$, U_p = 141 V, I_p = 110 A, P = 46 g. This increment of P may be considered as a consequence of electromagnetic acceleration of the plasma.

As a rule, the arcing voltage of the discharge decreased with the increase of filament voltage U_H of the cathode.

The experiments with the HTM (with lithium plasma) with ceramic side walls, molybdenum–rhenium cathode (δ = 1.2 mm), and tungsten anode (δ = 1.3 mm) showed that depending on the values of T_e, m, I_p, B_M, etc. three discharge regimes may be realized in the channel; these regimes are, respectively, characterized by: a) a single constricting arc and decreasing volt–ampere characteristic; b) a set of fine arcs, and oscillations of the current and voltage; c) distributed discharge and growing volt–ampere characteristic. The first and second regimes correspond to enhanced erosion of the material and disintegration of the electrodes; the resources of the models were short-lived. The regimes could be changed during the same experiment by changing the parameters; this caused the corresponding re-adjustment of the volt–ampere characteristics.

A stable electric discharge distributed over the surface of the electrodes was facilitated by a certain combination of a number of the above-mentioned factors; in particular, the increase in the flow rate and the temperature of the cathode generally improved the stability of the discharge. For T_e = 2500-2700°K and flow rate $\dot{m} \gtrsim 0.005$ g/sec a stable discharge could be obtained distributed over the entire area of the electrodes by varying B_M from 0 to 2000 G with average emission current density over the cathode j_* = 3-5 A/cm² (work function of Mo – Re $\varphi \approx 4$ eV). In the discharge the anode temperature T_α reached 2200-2600°K. (The values of T_c and T_α were practically constant along the channel.) Besides the temperature and probe measurements, a direct visual analysis of the surface of the electrodes also leads to the inference about the presence of a uniformly distributed discharge. The volt–ampere characteristics of the discharge (for $I_p \gtrsim 100$ A) were of the slightly growing type. They are shown in Fig. 4, where points 1-5 correspond to the following conditions: lithium, ceramic walls, $\dot{m}$ = 0.005 g/sec; 1) B_M = 1500 G; 2) 1300 G; 3) 1100 G; $\dot{m}$ = 0.006 g/sec; 4) 1300 G; 5) metallic walls, $\dot{m}$ = 0.005 g/sec, B_M = 1100 G.

In these experiments an increase of the flow velocity at the exit of the accelerator channel compared to the velocity at the end of the nozzle was also noted; the increase was

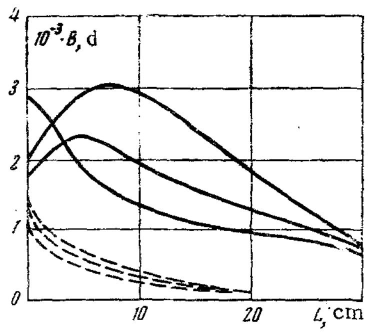

Fig. 2

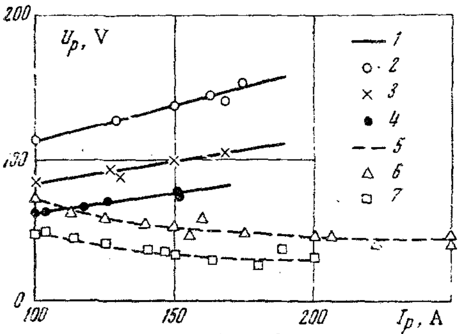

Fig. 3

from 6.5 km/sec (for the discharge power in the plasma source equal to 3.5 kW) to 13.5-22 km/sec, depending on the regimes of HTM I. This increase was a direct indication of the electromagnetic acceleration of the plasma. Thus, for $\dot{m}$ = 0.008 g/sec, B_M = 1100 G, T_c = 2500°K, T_a = 2600°K, I_p = 140 A ($j_* \approx 3$ A/cm²) the velocity recorded at the entrance was 6.25 km/sec, while the velocity at the exit was 12 km/sec; the measured reaction for the plasma source was P = 5 g, while for the accelerator it was 9.5 g.

The estimate of the flow velocity from the momentum and the rate of flow is in satisfactory agreement with the probe and spectroscopic measurements. The dependence of the flow velocity of the plasma on the magnetic field in HTM I is shown in Fig. 5; here points 1-4 are obtained in the following conditions: lithium, I_p = 140 A from probe measurements, $\dot{m}$ = 0.005 g/sec: 1) HTM I with metallic walls; 2) HTM I with ceramic walls; from momentum measurements, HTM I with ceramic walls; 3) $\dot{m}$ = 0.005 g/sec; 4) 0.008 g/sec.

The sum of the near-electrode drops ΔU_s (middle section of the channel) obtained from the probe measurements of the plasma potential is small compared to U_p; ΔU_s increases with B_M; for example, for $\dot{m}$ = 0.005 g/sec, $T_e = T_a$ = 2500°K, I_p = 140 A ΔU_s increased by ~28% on changing B_M from 1100 ($\Delta U_s \approx 8.5$ V) to 1500 G ($\Delta U_s \approx 11$ V); the heat flux q_w to the side wall (at the exit of the channel) as measured by calorimeter sensors also increased by 30% (from 0.12 to 0.16 W/cm²).

As expected, the increase of B_M resulted in an increase of U_p (Fig. 4). The reaction P also increased; thus, for the increase of B_M by a factor of 1.4 (from 1100 to 1500 G) with $\dot{m}$ = 0.005 g/sec (magnetic interaction parameter S changed from 25 to 60) P increased by a factor of 1.3. An increase of the flow rate from 0.005 to 0.008 g/sec had practically no effect on the qualitative dependence of P on B_M (for $\dot{m}$ = 0.008 g/sec S changed from 20 to 50), and the increase in P was again ~30%. The dependence of the reaction force of the lithium plasma jet on the magnetic field in HTM I is shown in Fig. 6 for I_p = 140 A; here points 1 and 2 correspond to $\dot{m}$ = 0.008 and 0.005 g/sec, respectively.

As the probe measurements showed, for the chosen profile of B (Fig. 2, curves 1-3) almost a uniform increase of the velocity was obtained over the basic length of the channel; larger acceleration was observed only in the initial segment of the channel $x/L \lesssim 0.15$. The distribution of T_e and n_e in the middle transverse section of the channel was recorded by five Langmuir probes; at the axis $T_e = 1.6\cdot10^4$°K, $n_e = 1.2\cdot10^{13}$ cm^{-3} ($\dot{m}$ = 0.008 g/sec, I_p = 140 A, T_c = 2500°K, T_a = 2600°K, B_M = 1100 G); T_e and n_e decreased in the direction of the electrodes.

On the basis of these experiments the HTM seem most recommendable from the point of view of the emission characteristics of the cathode made from MR47 alloy, which makes it possible to realize the regime of distributed discharge without impairing the durability of the electrode material j_* up to ~4 A/cm² (T_e = 2650°K). The absence of noticeable erosion of the electrodes was confirmed by the spectroscopic measurements. It was found that the nonisothermal nature of the plasma ($T_n/T_e \gtrsim 0.2$) was significantly smaller in the investigated models than in devices of the type discussed in [2, 3]. The cycle of necessary measurements determined the time of continuous operation of the HTM in each start-up, which reached ~1800 sec in most of the experiments.

4. Results of Experiments on Models with "Metallic" Walls

The investigations of models with ceramic side walls revealed a number of shortcomings resulting from the thermophysical characteristics of ceramic and by the direct contact of

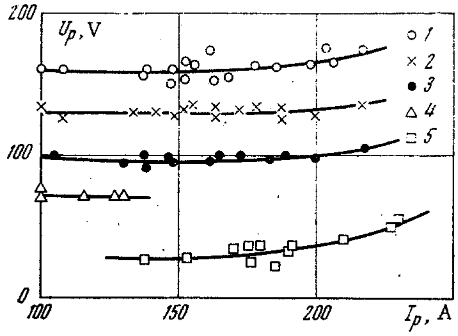

Fig. 4

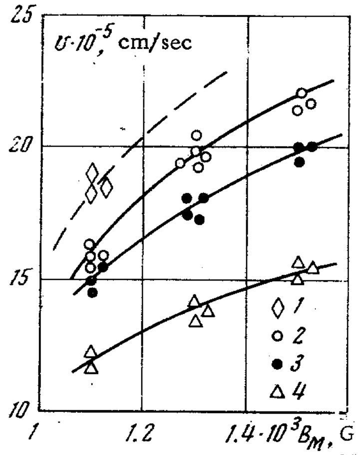

Fig. 5

the ceramic material with alkali plasma. On the one hand, the relatively low temperature of the inner surface of the walls ($T_W \lesssim 1000°K$ in the LTM and $T_W \lesssim 1400°K$ in the HTM) was the reason for not only partial condensation of the alkali metal (LTM), but also for the deionization of the plasma on their surface due to ambipolar diffusion of the charged particles and their subsequent recombination resulting in a decrease of the effective degree of ionization. On the other hand, in the HTM T_W was rather high for the normal operation of ceramics and caused a loss in its heat resistance. (The operating temperature of BNTs is $\lesssim 1500°K$.) In all cases the interaction of the aggressive alkali vapors with the ceramic impaired its electrical insulation properties and led to a gradual disintegration of the walls.

These contradictions were avoided and the problem of durability of the constructions was resolved by making metallic walls for the E,H-accelerators, consisting of ceramic base and high-melting metallic elements mounted on this base and insulated from each other [Fig. 7, 1) ceramic, 2) screens, 3) metallic elements]. In order to avoid shorting of Hall currents in the plasma the metallic walls were segmented not only along the height, but also along the length, of the channel. Due to special thermal screening these walls could have quite high temperature of the surface of the metallic elements swept by the plasma of the operating substance. The temperature of the ceramic was sufficiently low, the heat resistance was not impaired, and its interaction with the alkali plasma was almost eliminated. The resulting additional heating of the inner metallic surface of the walls improved the ionization state of the adjoining plasma, reduced the electron and ion losses, and eliminated the condensation of the vapors of the operating substance. In turn, the increased degree of ionization directly affected the efficiency of electromagnetic acceleration.

For a practical utilization of the metallic walls it was necessary to resolve the problem of maximum admissible potential difference in the gap between two adjacent elements arranged transverse to the electrodes, which would exclude the possibility of ruptures and current leakage into the wall. The investigation was carried out on models with a channel of constant cross section of 20 × 20 × 150 mm^3 and metallic walls having different number of transverse elements. Cesium vapor was used as the operating substance. The model operated in the regime of distributed discharge with film thermionic emission from a direct-channel tungsten cathode (T_c = 1300-1400°K) with density $j_* \lesssim 6$ A/cm^2 and time of continuous operation up to ~3000 sec. The anode was also of direct-channel type and made of tungsten (T_a = 1300-1400°K). The flow rate of cesium was $\dot{m}$ = 0.01-0.12 g/sec. The magnetic system ensured a field decreasing toward the exit with $B_M \lesssim 1500$ G.

The volt—ampere characteristics of the channel are shown in Fig. 8 for the case of cesium ($\dot{m}$ = 0.017 g/sec) with segmented transverse electrodes having four transverse elements (curves 1, 3 correspond to B_M = 600 G, B_M = 0) and continuous metallic walls (curve 2, B_M = 600 G).

It is evident that the volt—ampere characteristic consists of two branches separated by a zone of instability typical for electrical breakdwon. The arrows along the characteristics show the sequence of regulation of the discharge in time. The decrease of the current to a level, at which the volume discharge between the electrodes could be sustained in the absence of parasitic breakdowns in the gaps between metallic walls and the electrodes, led to the readjustment of the discharge and to transition from one branch of the volt-ampere characteristic to the other.

A comparison of the experimental results for different numbers of electrical discontinuities on walls 1 and 2 shows that curve 1 corresponds to the discharge without parasitic arcing along the wall. The voltage U_p at the point on curve 1, starting from which a sharp adjustment of discharge 2 occurs, should obviously be taken as the breakdown voltage. On this basis we obtained the relation between the critical breakdown voltage per gap between two transverse elements of the side wall (or an element and the electrode) and the ionization potential of the operating substance:

$$\Delta U_{cr} \approx 1.6 V_i$$

where V_i is the ionization potential of the operating substance.

The experimental investigations on the accelerator model operating on lithium showed that the fulfillment of the condition $\Delta U < \Delta U_{cr}$ would ensure the absence of breakdowns. Considerable attention was given to the investigation of regimes of heating of the walls. According to the computation the heat fluxes to the metallic walls (Fig. 7) on dielectric backing of BNTs have the upper bound $q_w \approx 10$ W/cm^2, which determines the maximum admissible operating temperature T_w^* of BNTs ceramic at ~1500°K; above $T_w \approx 1500$°K the thermophysical and mechanical characteristics of BNTs become noticeably impaired.

Experiments on heating of metallic walls of the LTM due to heating of the cathode (I_f = 780 A, U_f = 10 V) and anode (I_f = 885 A, U_f = 6.8 V) in a vacuum showed that there exists an appreciable temperature gradient between the operating surface of the metallic walls swept by the plasma and the inner surface of the ceramic due to screening. Thus, on heating the metallic elements up to T_m = 1525°K (T_m is the temperature of the metallic wall of the channel) T_w = 950°K (ΔT = 575°K). Thus, there exists a possibility of significant increase of T_m for $T_w < T_w^*$. The quality of insulation of the metallic walls against breakdowns was verified directly before assembling the models using a standard Megger. In spite of the heating of the walls in vacuum conditions, the presence of the external magnetic field facilitated maintenance of a high breakdown voltage for the appearance of surface discharges along the ceramic.

In the LTM with metallic walls tests were also conducted on a eutectic alloy of sodium and potassium, which has a larger vapor pressure compared to lithium (for avoiding condensation), and the heat capacity of preheating of the chamber was increased due to anode heating. With these measures the temperature T_m in the experiments could be maintained below 1000-1100°K, which corresponds to the measured heat flux $q_w \approx 6.5$ W/cm^2. In the central part of the walls T_m could reach ~1500°K in these series of experiments (I_p = 200-300 A), and T_w did

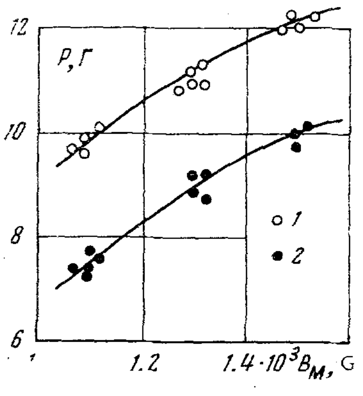

Fig. 6

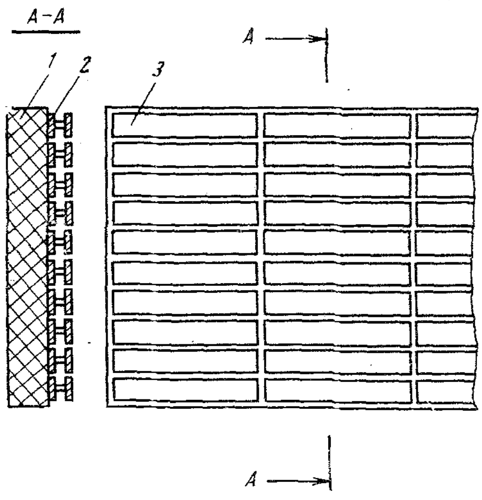

Fig. 7

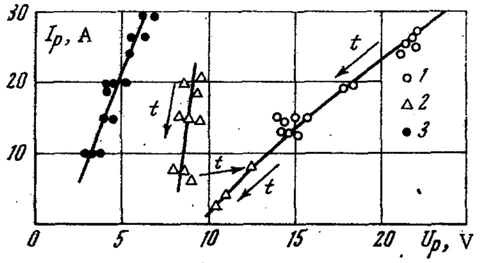

Fig. 8

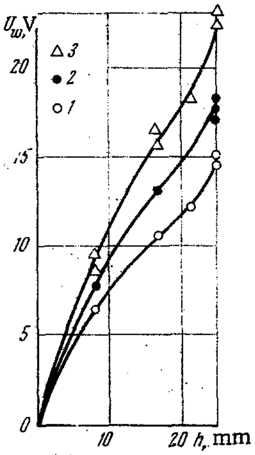

Fig. 9

not exceed 900°K. As a result the condensation of the operating substance inside the accelerator channel was completely eliminated, and a stable distributed discharge was obtained in the regime of thermionic emission of the cathode with growing volt—ampere characteristics [Fig. 3, 1) eutectic alloy of sodium and potassium, $\dot{m}$ = 0.02 g/sec; 4) solid anode, B = 0; 3) solid anode, B_m = 2350 G; 2) first segment of the anode, B_m = 2350 G]. The absence of the current leakage into the wall at a relatively large potential difference apparently indicates an efficient electrical resistance of the side walls.

In the investigated regimes at the exit T_e = 9000-12,000°K; for example, for $\dot{m}$ = 0.02 g/sec (Na—K), I_p = 130 A, U_p = 90 V (solid anode), B_m = 2350 G, T_e = 9000°K.

In HTM with the length of the cathode 200 mm (duration of start-up up to 3600 sec) the operating surface of molybdenum elements of the wall had T_m = 1800-2000°K, T_w = 1100-1400°K (the model was heated in vacuum for 1-2 h before the start-up). A direct result of using heated walls in HTM was the decrease in the voltage of discharge initiation (Fig. 4). Thus, in the presence of ceramic walls with $\dot{m}$ = 0.005 g/sec, B_m = 1100 G, I_p = 140 A, U_p = 100 V; if metallic walls were used for same $\dot{m}$, B_m, and I_p (T_e = 2700°K, T_a = 2400°K), the voltage decreased to ~30 V and the measured velocity increased to ~18.5 km/sec (Fig. 5).

This fact is explained by the increase of the degree of ionization of the plasma due to the increase in temperature of the layer near the wall and decrease of the recombination loss of the charged particles toward the periphery of the discharge. In this connection it is characteristic to note that the electron concentration near the metallic wall in the middle part of the channel increased to its level in the near-cathode plasma in the channel with ceramic walls. At a distance l = 2 mm from the metallic wall the recorded values were $n_e \approx 5 \cdot 10^{12}$ cm^{-3}, $T_e \approx$ 21,300°K; in the case of ceramic walls the values recorded near the cathode at a distance l = 2.5 mm were $n_e = 8 \cdot 10^{12}$ cm^{-3}, $T_e \approx$ 10,000°K (T_e = 2500°K, T_a = 2600°K, B_m = 1000 G, I_p = 140 A, $\dot{m}$ = 0.008 g/sec). In the case of use of lithium with $\Delta U < 1.6\ V_i$ the absence of current between two transverse elements of the wall was confirmed by direct measurements. In the process of operation of models with metallic walls information was obtained on the distribution of the potential U_w transverse to the metallic wall by measuring the floating potentials of the transverse elements of the wall with respect to the cathode (in the middle of the channel).

The mean distribution of the potential between the electrodes in the stationary stable regime of operation is characterized by a relatively smooth increase of U_w from the cathode to the anode. The distribution of the potential of the metallic wall transverse to the LTM channel is shown in Fig. 9. (cesium, $\dot{m}$ = 0.017 g/sec, curves 1-3 correspond to B_M = 600, 770, 920 G). Just as U_p, U_w increases with B_M.

On passing into the region of unstable regimes (for example, due to overloading $j_* >$ 6-7 A/cm² in the HTM) the development of low-frequency oscillations of the current and voltage (corresponding to the local micro-arc discharges on the background of the discharge of the model as a whole) appearing in the form of pulsations on the oscillograms (the amplitude of these pulsations generally did not exceed 0.1 of the main signal) was accompanied by synchronous oscillations of the measured wall potentials. The establishment of a stable diffuse discharge was accompanied by "smooth" oscillographic records of the current, voltage, and U_w. According to the measurements the voltage drop at the end transverse elements of the metallic wall was an appreciable fraction of the potential difference in the discharge.

The efficiency of the accelerators (without plasma source) increased considerably on changing over to metallic walls; in the single-stage scheme using eutectic alloy of sodium and potassium this increase was 15-30%. The efficiency of the two-stage accelerator exceeded that of the single-stage accelerator by more than a factor of two. An analysis of the operating process showed that an appreciable increase of the efficiency can be obtained by increasing the dimensions of the accelerator with corresponding increase in its power. Large dimensions of the channel must result in a decrease of heat losses from the plasma and the losses of the charged particles at the walls, as a result of diffusion (in relation to the rate of the process of bulk ionization).

Thus, the cycle of experimental investigations conducted here made it possible to obtain efficient acceleration of alkali plasma in an E,H-accelerator, whose scheme is distinguished by the high-temperature regime of the inner surfaces of the accelerator channel (with lithium $T_e \simeq T_\alpha = 2400\text{-}2700°K$, $T_M = 1800\text{-}2000°K$), relatively small divergence of the electron temperature $T_n/T_e \geq 0.2$, stable discharge distributed over a large area of the electrodes with current density up to ~6 A/cm^2, and Hall parameter in the channel $\omega_e\tau_e \sim$ 1-2.

The authors thank Yu. A. Tetyukhin, M. G. Shevtsov, V. G. Mikhalev, and B. S. Dimanov for participation in the experiments.

LITERATURE CITED

1. Plasma Accelerators [in Russian], Mashinostroenie, Moscow (1973).
2. V. I. Aref'ev and B. A. Khmelinin, "Anomalous heating of plasma by Hall current," Teplofiz. Vys. Temp., 10, No. 2 (1972).
3. V. I. Aref'ev and B. A. Khmelinin, "Investigation of plasma acceleration in crossed electric and magnetic fields," Teplofiz. Vys. Temp., 11, No. 4 (1973).
4. V. A. Zhirnov and A. V. Potapov, "Experimental investigation of a stabilized source of alkali metal, argon, and hydrogen plasma," in: Proceedings of the All-Union Conference on Physics and Low-Temperature Plasma Generators [in Russian], Alma-Ata (1970), pp. 410-413.
5. V. G. Pankratov, L. I. Zhulebin, and V. N. Stepanov, "Computation of the characteristics of a source of lithium plasma," Teplofiz. Vys. Temp., 9, No. 2 (1971).
6. O. N. Mironov, "Computational and experimental investigation of volt-ampere characteristics of a lithium plasma source," Izv. Sibirsk. Otd. Akad. Nauk SSSR, Ser. Tekh. Nauk, 1, No. 3, (1967).
7. O. V. Kozlov, Electrical Probe in Plasma [in Russian], Atomizdat, Moscow (1969).
8. Plasma Diagnostics [Russian translation], Mir, Moscow (1967).
9. A. P. Dronov, A. G. Sviridov, and N. N. Sobolev, "On measurement of flame temperatures by the method of relative intensities of spectral lines," Opt. i Spektrosk., 5, No. 5 (1958).
10. D. R. Bates and A. Damgaard, "The calculation of the absolute strengths of spectral lines," Philos. Trans. Roy. Soc. London, Ser. A. Math. and Phys. Sci., 242, No. 842 (1949).
11. V. A. Zhirnov and Yu. A. Tetyukhin, "Problem of determining electron concentrations in lithium plasma by a spectroscopic method," Zh. Prikl. Spektrosk., 18, No. 4 (1973).